ICAS 2016
30th Congress of the International Council of the Aeronautical Sciences
DCC, Daejeon, Korea ; September 25-30, 2016

A STUDY ON FAILURE BEHAVIORS OF REPAIRED COMPOSITE STRUCTURES WITH SCARF BONDED PATCH

Khanh-Hung Nguyen, Viet-Hoai Truong, Jin-Hwe Kweon*
School of Mechanical and Aerospace Engineering, Research Center of Aircraft Part Technologies, Gyeongsang Natinal University, Jinju, Gyeongnam 660-701, South Korea

Keywords: *composite repair, damage zone method, failure prediction, scarf bonded joint*

Abstract

The damage zone method (DZM) is an efficient way to predict the failure of composite structures with a minimum number of test. Particularly, it is useful when the failure mechanism is too complicated to be accurately analyzed by a merely finite element method. The aim of this study was to use the damage zone model to predict the failure load of repaired laminates, in which scarf bonded joints were used for repair. The model uses a test-based critical damage zone and stress-based failure criteria. A total of 45 carbon-epoxy composite (USN) laminate scarf-repaired specimens were first tested with 2 different defect sizes, 4 scarf angles and 3 overlap layer sizes. The Tsai-Wu and Tsai-Hill criteria were used for the laminate, and the maximum shear stress criterion for the adhesive was adopted to predict failure onset. The predicted failure loads were compared to test results and a good agreement was obtained with a 9.2% maximum deviation for almost all parameters with the exception of a case with an unrealistically large scarf angle.

1 Introduction

Bonded composite repairs are increasingly used to repair composite structures because of their high strength recovery and lack of stress concentration due to fastener holes. Adhesive bonded composite patch repair is a valuable repair method used to restore the structural integrity of a damaged part. In addition, laminate patch repair is a local repair method and is more common than replacing the whole damaged laminate for economic and mechanical reasons. The partially damaged laminate is first removed in the form of circular or rectangular cutouts. To restore its shape and strength, the open cutout is repaired by adding an adhesive bonded patch. Several types of bonding joints, such as over-lap, stepped-lap and scarf-lap, can be used to join the cutout composite to the patch. As a result, the strength of the repaired laminate is commonly equal to the strength of the bonded joints that were used for the repair. Hence, it is clear that an understanding of the failure behaviors and methods of predicting failure load for adhesive bonded joints is necessary to investigate those of the repaired laminates.

The strength of an adhesive bonded joint is generally influenced by many factors such as the adhesive and adherend materials, the overlap length and the quality of bonding surfaces. To achieve the full strength of an adhesive, the failure mode should be a cohesive one and not interfacial one. Adhesive bonding is extremely sensitive to the surface preparation process and interfacial failure can easily be caused by a small error in the fabrication procedures. Consequently, the strength of an adhesive joint may vary depending on the manufacturing quality.

To correctly design an adhesive bonded joint and to take full advantage of adhesive bonding in industrial applications, the failure modes and the strength of the joint need to be predicted accurately. The principal failure modes in this type of joints are (i) cohesive failure (failure of adhesive material), (ii) interfacial failure and (iii) adherend or substrate failures.

In terms of bonded joints, most published studies are related to single lap joints and the finite element method (FEM). The viability of the FEM for design and analysis has improved considerably with the recent and rapid development of computing technology. The

FEM presents the possibility of building models which are very close to the structures investigated. Several studies use finite element analysis to predict the strength of adhesive bonded joints [1,2]. Adams et al. [3] proposed a method to predict failure loads by using a plane strain, geometric and material nonlinear finite element analysis. The authors assumed that the failure occurs when the maximum principal stress or strain at one Gauss point close to the end of the overlap area exceeds the allowed value for the corresponding material. However, their approach depends strongly on the refinement of the finite element mesh.

Another method was proposed by Crocombe [4] to predict the bond line failure of single lap joints. Here, it was assumed that the failure occurred when the whole adhesive layer became plastic. This method is unreliable for bonded joints, where local failure can occur before global yielding rather than after adhesion fails. It was shown that bonded joint failure could be predicted when the maximum principal stress over a finite zone in the adhesive exceeded the ultimate tensile stress of the adhesive [5]. Meanwhile, John [6,7] believed that the failure of bonded composite joints occurs when the adhesive exceeds the shear stress allowable in a critical portion of the joints.

A damage zone method (DZM) was developed from Crocombe's method by Sheppard and Kelly [8] to predict the failure of aluminum and graphite/epoxy composite adhesive bonded joints. Their prediction showed a good agreement with experimental results that used the adhesive peel strain failure criterion. The method was not sensitive to mesh size and was very applicable to industrial problems. Prior to analysis, the method required at least one test to evaluate the critical damage zone value. This critical value was then applied to predict failure loads of other joints.

The damage zone model based on 3D finite element analysis was then used by Nguyen et al. [9] to predict the failure load of single lap joints with dissimilar adherend materials. A resin layer with one-tenth the thickness of a composite lamina was inserted between any two adjacent orthotropic layers in their model. The Ye and Von Mises strain criteria were applied to out of plane adherend failure and adhesive failure, respectively. The predicted results were in good agreement with experiment for nine different bonding lengths and adherend thicknesses.

Scarf bonded joints have also been investigated by several researchers. The effects of many parameters such as laminate and adhesive thicknesses, overply laminate and scarf angle on strength of scarf bonded joints were investigated using 2D and 3D linear finite element analysis [10]. A new 2D plane stress model, developed from the traditional 2D plane stress model, was proposed by Randolph et al. [11] and was applied to modeling scarf bonded joints. The study focused on the effects of scarf angles on the failure load of the joints, and the failure load prediction was in good agreement with the experimental results, with the exception of the two smallest scarf angles joints.

In a parametric study on circular scarf joints, Pinto et al. [12] conducted a 3D circular patch analysis with cohesive zone models to simulate damage onset and growth in the adhesive layer. Trapezoidal cohesive laws were also used to account for the ductility of the adhesive used. In the article, the width of adherends and the scarf angle were studied in detail. In addition, the use of over-laminate plies to cover the repaired region was tested to improve the repair efficiency. This parametric study allowed the proposal of design principles for the repair of composite structures. A failure load prediction, however, was not proposed.

According to the above literature survey, the method of failure load prediction has not been well defined for adhesive bonded joints in general and scarf bonded joints in particular. The applicable area and accuracy of the published methods also need to be improved, and therefore more studies in failure load prediction of scarf bonded joints are necessary.

The main aim of this work was to predict the failure load of a laminate repaired by scarf bonded joints using DZM with several failure criteria. A 3D finite element analysis was performed using the commercial MSC.Nastran finite element code. Nine carbon-epoxy unidirectional repaired laminates were manufactured with different joint design parameters: scarf angle, over-lap length and

defect size were tested. The strength of the adherend without a patch was first compared to the shear stress in the adhesive based on the scarf angle, first to find the weakest part, and then to predict the failure modes of scarf bonded joints. The predicted failure load was also compared to the test results to evaluate the accuracy of the prediction. Besides, to verify the feasibility of the DZM for different material, additional 30 repair specimens using other carbon-epoxy unidirectional-laminate were tested and the accurate predictions were confirmed by the results of the experiment.

2 Test

2.1 Specimen preparation and testing

A schematic configuration of the repaired laminate is shown in Fig. 1. To protect the patch tips and increase the strength of the repairs, two woven fabric plies (WSN-3K) with a stacking sequence of [0/90] were bonded over the repaired region, as shown in the figure. The detailed geometry of the repaired laminates is given in Table 1. Figure 2 shows the typical repaired specimens.

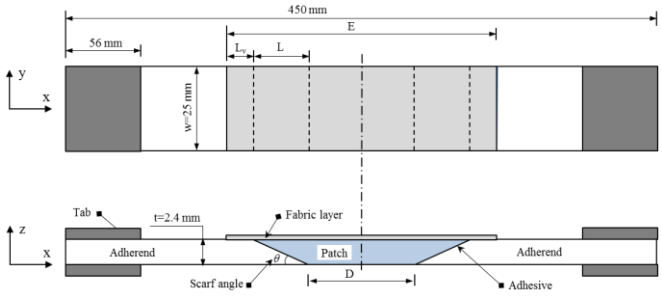

Fig. 1. Schematic configuration of repaired laminate used for tensile testing.

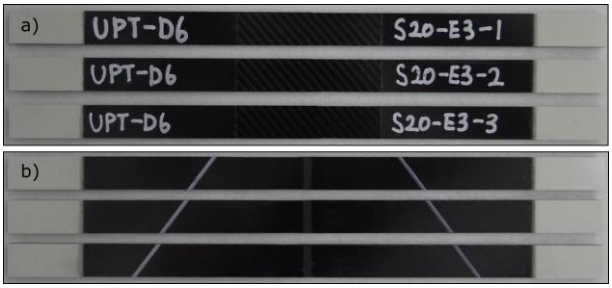

Fig. 2. Typical repaired specimens after repair (C2-2)

(a) Front view (b) Back view

A tensile test was conducted according to ASTM Standard D3039/D3039M (Fig. 3). Load was applied with a constant head displacement rate of 1.27 mm/min. Failure is defined as the maximum load in the load-displacement curve.

Table 2 shows the material properties of carbon-epoxy fabric (WSN-3K) and carbon-epoxy unidirectional prepregs (USN-125B) [13]. Nominal ply thickness of USN-125B and WSN-3K are 0.12 mm and 0.16 mm, respectively. For measuring the mechanical properties of the film adhesive, a test was also conducted and its material properties are given in Table 3.

Table 3. Material properties for adhesive

Spec. ID	Scarf angle (degree)	Scarf length L(mm)	Scarf ratio S	Overply lap length L_v(mm)	Defect size D(mm)	Patch size E (mm)
A11	11.3	12	5	5	6	40
A5-1	5.7	24	10	5	6	64
A5-2	5.7	24	10	5	12	70
C2-1	2.9	48	20	5	6	112
C2-2	2.9	48	20	3	6	108
C2-3	2.9	48	20	7	6	116
C2-4	2.9	48	20	5	12	118
C1-1	1.9	72	30	5	6	160
C1-2	1.9	72	30	5	12	166

2.2. Test results

All test results were reported in Yoo et al. [13] and therefore are only briefly described here. As shown in Fig. 4, the load-displacement curves of the A5-1 and C2-1 specimens under tensile loading are fairly linear up to final failure. The test results are summarized in Table 4 [13]. As shown in Table 4, the failure load increases with a decrease in scarf angle.

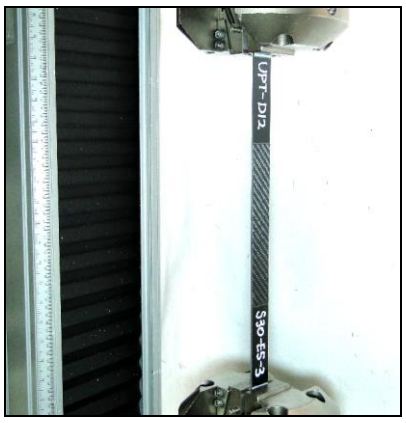

Fig. 3. Test set-up.

Table 2. Material properties of prepreg

Symbol	USN-125B	WSN-3K
E_1(Gpa)	142	70
E_2(Gpa)	8.4	70
E_3(Gpa)	8.4	9.6
G_{12}(Gpa)	5.34	3.59
G_{13}(Gpa)	5.34	-
G_{23}(Gpa)	3.06	-
ν_{12}	0.298	0.058
ν_{13}	0.298	-
ν_{23}	0.47	-
X_T (MPa)	2320	959
Y_T (MPa)	37.6	959
Z_T (MPa)	37.6	-
X_C (MPa)	1400	-
Y_C (MPa)	130	-
S_{12}(MPa)	82.3	119
S_{13}(MPa)	82.3	-
S_{23}(MPa)	40	-
T(mm)	0.120	0.160

Two main failure modes were observed in the experiment and are illustrated in Fig. 5 : (i) Mode A (A5-1): failure is dominated by cohesive failure in the adhesive film with little or no laminate fracture (ii) Mode B (C1-1): failure is dominated by laminate fracture. The existence of failure mode B verifies that the adhesive is not always the weakest part in the scarf joints, and agrees with published results [14,15].

Table 3 Material properties of adhesive

Property	Symbol	Value
Young's modulus (MPa)	E	3500
Shear modulus (MPa)	G	1268
Shear strength (MPa)	τ_p	40
Poisson's ratio	ν	0.38

3 Prediction of Failure Load Using the Damage Zone Method

The finite element model was created in MSC.Patran software by using three-dimensional elements. As the arrangement is symmetric about the *xz* and *yz* planes, the finite element models are confined to the quadrant of the laminate where the *x* and *y* values are positive. Symmetry restraints were applied across the *xz* and *yz* planes, as shown in Fig. 6. The failure load was then predicted using the stress results from analysis.

Table 4 Test results

Spec. ID	Scarf angle	Failure load (kN)			Failure mode
		Min	Max	Ave.	
A11	11.3°	9.2	10.8	10.2	Combined failure
A5-1	5.7°	24.8	28.3	26.1	Dominated by cohesive failure
A5-2	5.7°	25.7	29.2	27.8	
C2-1	2.9°	39.7	41.3	40.6	Dominated by laminate failure
C2-2	2.9°	35.0	38.3	36.8	
C2-3	2.9°	36.6	39.6	38.3	
C2-4	2.9°	39.8	41.7	40.7	
C1-1	1.9°	42.0	44.3	42.8	
C1-2	1.9°	40.2	41.1	40.6	

3.1 Finite element model

Nine finite element models were constructed, and represented nine different geometries of the repair patches with three parameters: overply lap length, defect size and scarf angle. The models consisted of twenty-layered composite laminates for the adherends and the repair patch was bonded by an adhesive placed along a scarf. Individual plies were discretely modeled for both adherend and patch. The models were meshed with the linear hexahedral elements. As shown in Fig. 7, a refined finite mesh was used for the interface region along the bonded line to accurately predict the stress and strain values while the other areas have a coarser mesh. The composite prepregs were considered to be anisotropic materials. Perfect adhesion was assumed between the adhesive and the adherend.

After linear static analysis, six stress components of the elements were reported to evaluate the failure using maximum shear stress, Tsai-Hill and Tsai-Wu failure criteria. The DZM was then used to predict failure loads for the joints based on a total volume of failed elements in a specific region.

3.2. The damage zone method

The DZM is based on the assumption that failure will occur after an appropriate number,

area or volume of elements failed in the finite element model.

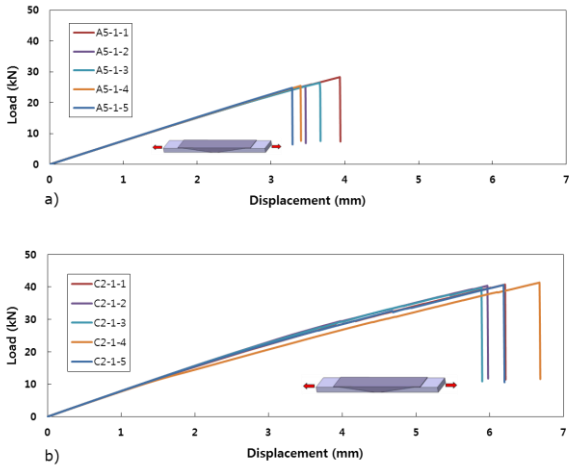

Fig. 4. Load-displacement curves of A5-1 (a) and C2-1 (b) repaired laminates.

The following is an outline of the procedure used to predict the failure load using DZM:

(i) Test one or more reference specimens and record the failure loads and failure modes.

(ii) Apply the tested failure load of the reference specimens to the finite element model and evaluate the critical damage zone corresponding to the tested failure load.

(iii) Use the critical damage zone calculated in the previous step to predict the failure load of other specimens.

In this study, the DZM was applied to predict the failure load of a repaired laminate with scarf bonded joints. This approach assumes that the specimen fails when the damage zone inside it exceeds that critical value [8,9]. In other words, the specimen fails when Eq. (1) is met:

$$DA = CDA \tag{1}$$

in which,

$$DA = \frac{DV}{L} \tag{2}$$

where *DA*, *CDA*, *DV* and *L* are damage zone, critical damage zone and volume of the damaged elements in the model and scarf length, respectively. It should be noted that the damage zone includes the effect of geometry change as reported in [8, 9].

In this work, an A5-1 laminate was first randomly selected as the reference (any model can be selected as the reference). The average failure load of the A5-1 laminate (26.1 kN) was then applied to the finite element model. As mentioned above, the maximum shear stress failure criterion was selected to define the failure of adhesive layer. The volume of all failed elements inside this reference model was then calculated to determine a critical damage zone. The damage zone grows in size with an increase of the applied load.

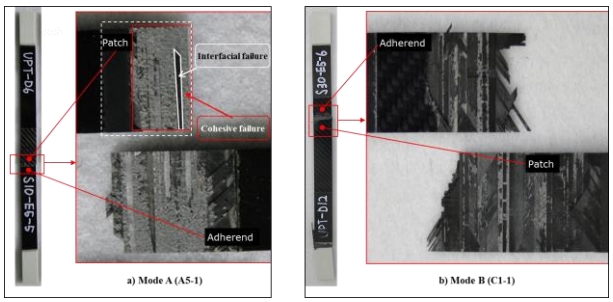

Fig. 5. Two main failure modes observed from experiment (a) Mode A: failure dominated by cohesive failure in an adhesive film with little or no laminate fracture (A5-1) (b) Mode B: failure dominated by composite adherend fracture (C1-1).

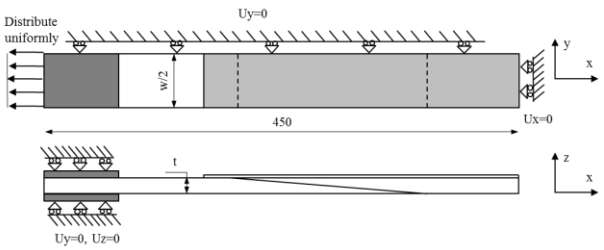

Fig. 6. Boundary conditions for the finite element model.

However, our preliminary analysis shows that if only one critical damage zone is used for all repaired laminates that have different geometries, the failure load was not well predicted because the failure modes depend greatly on the specimen geometry. Hence, in this study, two specimens were chosen as the reference specimens. The first reference specimen refers to the specimen that failed under cohesive failure mode and the other refers to the failure of laminated parts (both adherends and patch).

In terms of the effect of joint geometry on the failure mode of scarf bonded joints, previous

works [14-16] reveal that the failure mode is related to the scarf angle in scarf bonded joints. As seen in Fig. 8, a uniform shear stress and the normal stress in an adhesive layer are given by Eqs. (3.1) and (3.2), respectively:

$$\tau_p = \frac{P \sin\theta \cos\theta}{t} \tag{3.1}$$

$$\sigma_T = \frac{P \sin^2\theta}{t} \tag{3.2}$$

where τ_p, σ_T, P and θ are the shear stress and normal stress in the adhesive layer, distributed load and scarf angle, respectively. The adhesive was assumed to undergo only elastic shear stress/strain behavior.

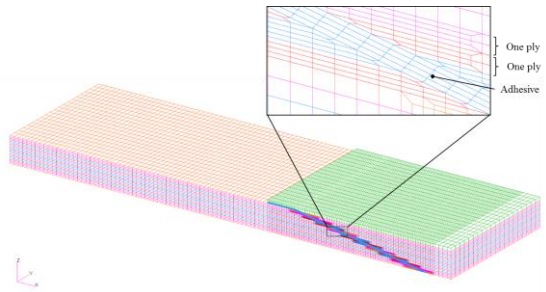

Fig. 7. Finite-element mesh.

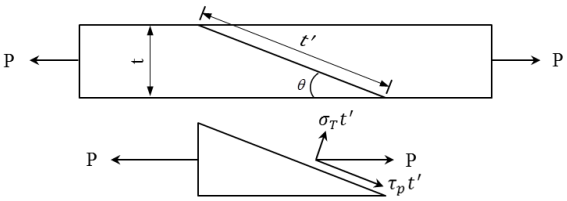

Fig. 8. Scarf angle limiting.

Thus, for a small scarf angle, the normal stresses are negligible. According to Alan Baker [14], the adherend fails before the adhesive yield when Ineq. (3.3) is met:

$$P_{Max} = \sigma_u t \le \frac{\tau_p t}{\sin\theta \cos\theta} \tag{3.3}$$

Thus:

$$\theta \le \frac{\tau_p}{\sigma_u} \tag{3.4}$$

In this study, a scarf angle limiting, $\theta_{\lim}$, with considering the effect of the external plies on the repaired laminate strength, was defined by Eq. (4).

$$\theta_{\lim} = K_e \frac{\tau_p}{\sigma_u} \tag{4}$$

in which,

$$K_e = \frac{t + t_e}{t} \tag{5}$$

where τ_p, σ_u, K_e, t and t_e are the shear strength of the adhesive layer, the strength of laminate adherend without a patch, ratio affected by the external plies, laminate thickness and external plies thickness, respectively. In this study, τ_p and σ_u have the value of 40 MPa and 853.3 MPa, respectively. The scarf angle limiting, $\theta_{\lim}$, is calculated to be 3.0° by Eq. (4).

A prediction of failure mode based on the scarf angle limiting was proposed. It is believed that this failure mode is dominated by cohesive failure in the adhesive film with little or no fracture of the composite adherends (mode A) when the scarf angle is larger than the scarf angle limiting, while the smaller scarf angle failure is dominated by laminate fracture (mode B).

From the scarf angle limiting, A11 (11.3°) and two A5 (5.7°) type laminates with the larger scarf angle were categorized into the large scarf angle group with failure mode A, while the others were categorized into the small scarf angle group with failure mode B. The failure load of the two groups need to be predicted separately based on two different critical damage zones, CDA_A and CDA_B which were calculated for specimens showing failure modes A and B, respectively.

3.3 Failure criteria

In the damage zone model, failure criteria are required to determine damage zones. The damage zone is identified by marking the failed elements. It is necessary to find suitable failure criteria to predict the joint strength when a combination of adhesive and composite adherend failure modes is present. The failure of adherend and adhesive layer is considered

separately in this study. The failure of the adherend was investigated using Tsai-Wu and Tsai-Hill criteria, while the maximum shear stress criterion was applied to the adhesive layer.

Several failure criteria, such as maximum shear stress, Von Mises stress and Von Mises strain, were also applied to the adhesive layer to identify the failed element inside it. These Von Mises criteria, however, did not result in a good prediction of the failure load compared to the maximum shear stress and are not reported in the current study.

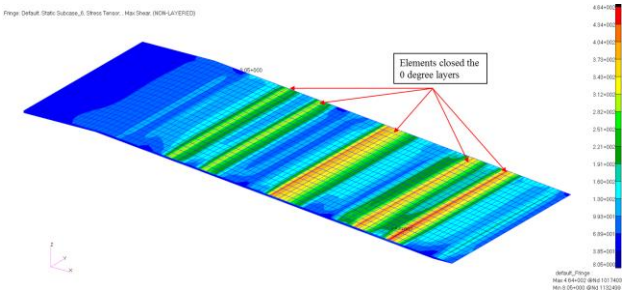

Fig. 9. Shear stress distribution in the adhesive layer of A5-1 model.

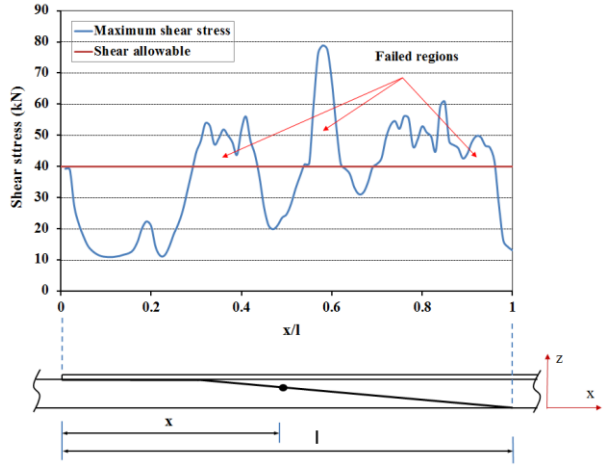

Fig. 10. Distribution of maximum shear stress in the adhesive layer of A5-1 repaired laminated along the *x*-direction at the mid-plane (*y*=0).

3.4 Prediction of failure load and failure mode

As mentioned in the previous section, the type of failure mode affects the strength of scarf joints in the repairs. Two predicted failure modes based on the calculation of the scarf angle limiting were in line with the test results for most cases with the exception of the A11 repaired laminate.

Figure 9 shows the shear stress distribution in the adhesive layer of the A5-1 model which was selected to be the reference model for the large scarf angle group. As seen in this figure, the shear stress is highest in locations close to each 0 degree layer. This analysis result was consistent with results of Pinto [12].

Table 5. Predicted fail. load of large scarf angle group by DZM using Max. shear stress criterion for adhesive

Spec. ID	Fail. Load (kN)	Damage zone		Predicted load(kN)	Error (%)
		DV	*DA*		
A5-1	26.1	23.7	0.98	26.1	0.0
A5-2	27.8	25.8	1.08	26.2	5.8
A5-3	10.2	1.5	0.43	14.1	38.2

Figure 10 shows the shear stress distribution in the adhesive layer along the *x*-direction on symmetric plane *xz* (y = 0) under an applied load. Here, the adhesive layer length l is a sum of the scarf length L and the overply lap length L_v, and has a value of 29 mm. The figure reveals that several regions in adhesive layer, where the shear stress is higher than the allowable shear stress, fail.

Table 5 summarizes the results of the failure load prediction for the large scarf angle group using DZM and the maximum shear stress failure criterion. The damage volumes, damage zones and critical damage zone are listed in the table. The A5-1 repaired laminate was chosen as a reference specimen to predict the failure loads of other laminates in the large scarf angle group using DZM. The critical damage zone for this group CDA_A was calculated to be 0.98 mm^2. The predicted failure loads were calculated based on this critical damage zone and were subsequently compared with test data. This table also shows that the damage zone of the A5-2 laminate was higher than the critical damage zone. As a result, the predicted load of this repaired laminate is lower than the tested failure load. Figure 11 elucidated the deviation between the predicted failure loads using DZM for the laminates in the large scarf angle group and the tested failure loads. As observed in the figure, the predicted failure load of the laminate with the largest scarf angle joint A11 is 14.1 kN, which is 38.2% higher than the test result.

Table 6. Failure load predicted for the small scarf angle group by DZM using the Tsai-Hill failure criterion for adherend

Spec. ID	Fail. Load (kN)	Damage zone *DV*	Damage zone *DA*	Predicted load(kN)	Error (%)
C2-1⁎	40.6	1305	27.19	40.6	0
C2-2	36.8	1265	26.35	42.6	15.7
C2-3	38.3	1310	27.29	38.1	0.6
C2-4	40.7	1389	28.94	37.9	6.9
C1-1	42.8	1983	27.54	40.2	6.1

Note: ⁎ Reference specimen

Table 7. Predicted failure load of the small scarf angle group by DZM using Tsai-Wu failure criterion for adherend

Spec. ID	Fail. Load (kN)	Damage zone *DV*	Damage zone *DA*	Predicted load(kN)	Error (%)
C2-1⁎	40.6	1150	23.96	40.6	0
C2-2	36.8	1112	23.17	40.2	9.2
C2-3	38.3	1157	24.10	37.8	1.3
C2-4	40.7	1214	25.29	37.6	7.6
C1-1	42.8	1713	23.79	45.6	6.5

Note: ⁎ Reference specimen

The lower accuracy of the prediction for the A11 repaired laminate is primarily due to an additional failure mode on the surface. Figure 12 shows that the failure mode for the A11 laminate is a combination of cohesive and interfacial failure modes. The interfacial failure mode occurred frequently in the failure surfaces for these samples, but was seldom or never observed for the other repaired laminates in the large scarf angle group. In other words, the presence of interfacial failure considerably affected the strength of adhesive bonded joints and, as a consequence, the strength of the repair, as well as the accuracy of predicted failure loads.

This complicated laminate failure mode could be related to the low quality of bonding surface preparation. During the manufacturing process, we found that the A11 laminate was much more difficult to manufacture than the others because its bonding surface is too sloping and short. This was also reported in a similar study of scarf bonded joints by Adkins [15]. The manufacturing of a joint with a large scarf angle could easily affect the quality of bonding and lead to interfacial failure.

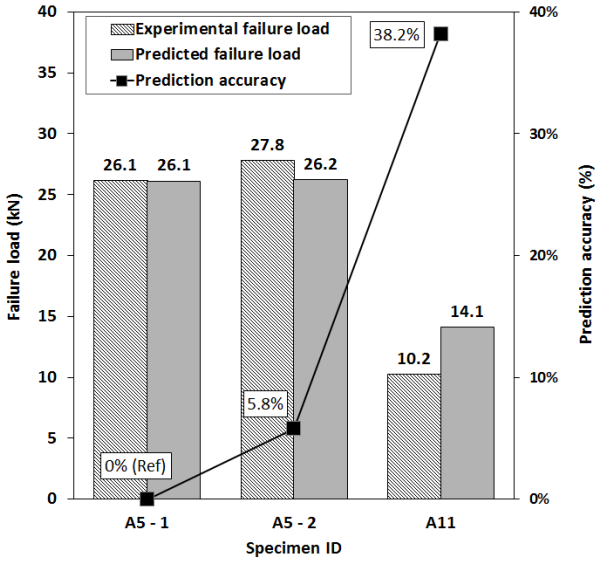

Fig. 11. Predicted failure load for the large scarf angle group using DZM and the maximum shear stress failure criterion for the adhesive.

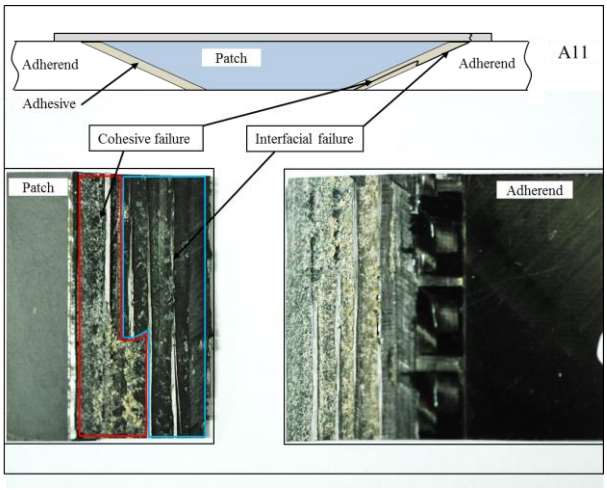

Fig. 12. Failure mode of A11 repaired specimen: Combined cohesive and interfacial failure.

Similarly, results for the failure load prediction of the small scarf angle group using DZM and the Tsai-Hill failure criteria are summarized in Table 6. The damage volumes, damage zones and critical damage zone are listed in the table. The C2-1 laminate was chosen to be the reference specimen for predicting failure loads of other laminates in the small scarf angle group using DZM. The critical damage zone for this group CDA_B was calculated to be 27.19 mm^2. The predicted failure loads were calculated based on this critical damage zone and subsequently compared with test data. This table also shows

that the damage zone for the C2-2 laminate was lower than the critical damage zone. As a result, the predicted load of this repaired laminate is higher than the tested failure load. The predicted failure loads for the small scarf angle group by DZM with the use of Tsai-Hill criterion for the adherend are compared to the tested failure loads in Fig. 13. The figure indicates that the predicted failure loads differed slightly from the corresponding tested failure loads, with a maximum deviation of 15.7%.

Similarly, the prediction using the Tsai-Wu failure is given in Table 7. A good prediction of failure loads was achieved, and the maximum deviation was reduced to just 9.2%, as shown in Fig. 14.

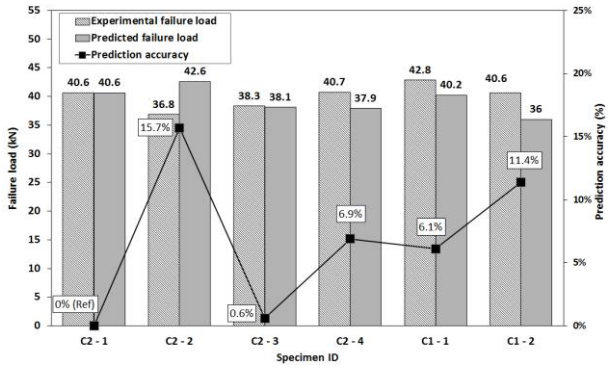

Fig. 13. Failure load predicted for the small angle group by DZM using the Tsai-Hill failure criterion for the adherend

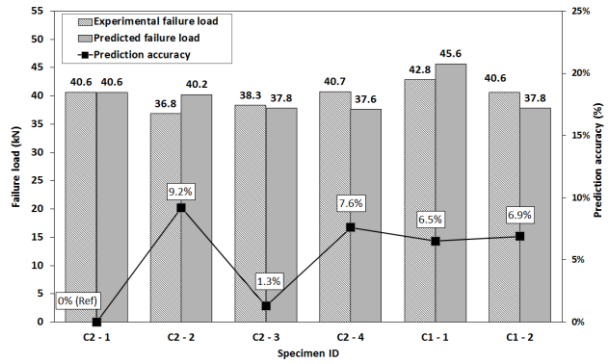

Fig. 14. Predicted failure load of the small scarf angle group by DZM using the Tsai-Wu failure criterion for adherend

4 Conclusions

From this study examining the failure load prediction of repaired laminates using DZM, the following can be concluded. First, two main failure modes were predicted based on the scarf angle limiting which is calculated separately from the strength of adhesive and adherend parts and was in good agreement with test results. It is believed that the proposed scarf angle limiting can be used for prediction of failure mode of the scarf-patch repair with various joint geometry and materials. Second, the results confirm the feasibility of using small angles for the scarf repair because adhesive is not always the weakest part in the small scarf angle joints. In addition, it is possible to accurately predict the failure load of repaired laminates with scarf bonded joints if a suitable failure criterion is applied. Finally, using this method, the failure load of repaired laminates could be predicted to within 15.7% for virtually all cases, even though published papers reveal that there is no universally accepted procedure to accurately predict adhesive bonded joint strength. Especially, the use of Tsai-Wu failure criterion resulted in a maximum deviation of 9.8% from experiment with the exception of the largest scarf angle (11.3^{o}) repaired laminate A11. The prediction for this repaired laminate, however, was not very reliable because of the presence of a combined adhesive and cohesive failure mode which usually happens in the manufacturing of scarf bonded repairs with a large angle.

5 Acknowledgements

This study was supported by the "Advanced Scarf Repair Method and Equipment Development for Aircraft MRO" through the Ministry of Trade, Industry and Energy (R0004399-2) and the "Next-Generation Mechanical and Aerospace Creative Engineers Education Program" (BK21 PLUS Project) at Gyeongsang National University, Korea..

References

[1] Kumar, S.B., Sridhar, I., Sivashanker, S., Osiyemi, S.O., Bag, A.: Tensile failure of adhesively bonded CFRP composite scarf joints. Mater. Sci. Eng., B. 132, 113-120 (2006)

[2] Rahman, N., Roh, H.: Prediction of Failure Strength of Adhesive Joints Using Peel stress and CTOA. Conference: 52nd AIAA/ ASME/ ASCE/ AHS/ ASC Structures, Structural Dynamics and Materials Conference 19th, At Denver, Colorado, Volume: AIAA 2011-1720.

[3] Harris, J.A., Adams, R.D.: Strength prediction of bonded single lap joints by nonlinear finite element methods. Int. J. Adhes. Adhes. 4(2), 65-78 (1984)

[4] Crocombe, A.D.: Global Yielding as a Failure Criterion for Bonded Joints. Int. J. Adhes. Adhes. 9, 145-153 (1989)

[5] Clark, J.D., McGregor, I.J.: Ultimate tensile stress over a zone: A new failure criterion for adhesive joints. J. Adhes. 42(4):227-245 (1993)

[6] John, S.J.: Predicting the strength of bonded carbon fibre/epoxy composite joints. In: Damico, D.J., Wilkinson, T.L., Niks, S.L.F., editors. Composites bonding, ASTM STP 1227. Philadelphia: ASTM, 45-59 (1994)

[7] John, S.J., Kinloch, A.J., Matthews, F.L.: Measuring and predicting the durability of bonded carbon fibre/epoxy composite joints. Composites Part A. 22(2):121-126 (1991)

[8] Sheppard, A., Kelly, D., Tong, L.: A damage zone model for the failure analysis of adhesively bonded joints. Int. J. Adhes. Adhes. 18, 385-400 (1998)

[9] Nguyen, K.H., Kweon, J.H., Choi, J.H.: Failure load prediction by damage zone method for single lap bonded joints of carbon composite and aluminum. J. Compos. Mater. 43(25):3031-3056 (2009)

[10] Gunnion, A.J., Herszberg, I.: Parametric study of scarf joints in composite structure. Compos. Struct. 75, 364-376 (2006)

[11] Randolph, A.O., Clifford, M.F.: An improved 2D model for bonded composite joints. Int. J. Adhes. Adhes. 24, 389-405 (2004)

[12] Pinto, A.M.G., Campilho, R.D.S.G., de Moura, M.F.S.F., Mendes, I.R.: Numerical evaluation of three dimensional scarf repairs in carbon-epoxy structures. Int. J. Adhes. Adhes. 30(5), 329-337 (2010)

[13] Yoo, J.S., Truong, V.H., Park, M.Y., Choi, J.H., Kweon, J.H.: Parametric study on static and fatigue strength recovery of scarf-patch-repaired composite laminates. Compos. Struct. 140, 417-432 (2016)

[14] Baker, A.: Composite materials for aircraft structures. Published by American Institute of Aeronautics and Astronautics, Inc. 1801 Alexander Bell Drive, Reston, VA 20191-4344.

[15] Pipes, R.B., Adkins, D.W.: Strength and repair of bonded scarf joints for repair of composite materials. Center for Composite Materials, College of Engineering University of Delaware (1982)

[16] Adkins, D.W., Pipes, R.B.: Tensile behavior of bonded scarf joints between composite adherends. Proceedings of the fourth Japan-US Conference on Composite Materials, 845–854 (1988)

6 Contact Author Email Address

The corresponding author of this paper is Prof. Jin-Hwe Kweon (mailto: jhkweon@gnu.ac.kr)

Copyright Statement